Computer Modelling of Close-to-Ground Tornado Wind-Fields for Different Tornado Widths

M. Hossein Kashefizadeh
BELL 4190 University of Arkansas
Fayetteville, AR 72701, USA
email: mkashefi@uark.edu

Sumit Verma
BELL 4190 University of Arkansas
Fayetteville, AR 72701, USA
email: sv015@uark.edu

R. Panneer Selvam*
BELL 4190 University of Arkansas
Fayetteville, AR 72701, USA
email: rps@uark.edu

*Corresponding Author

Abstract

Tangential velocity (V_t) of tornadoes is the major parameter that causes building damage. In-field tornado measurements are less reliable at less than 20m above ground level (AGL). Laboratory tornado simulators suggest that swirl ratio (S) and radius (r_o) are the major tornado parameters that influence the V_t. However, due to scaling problems, the laboratory simulators also report the V_t at greater than 20m AGL. Well-refined computational fluid dynamics (CFD) models can evaluate the V_t at less than 10m AGL. However, the CFD models are limited to r_o=1.0km, and the effect of r_o on the V_t is not investigated. The aim of this study is to investigate the maximum V_t for different r_o close to ground. Simulation results show that increasing r_o decreases the maximum V_t with respect to V_{ro}. Moreover, by increasing ro, the corresponding elevation of occurrence of maximum Vt (zmax) will increase. However, for all tornado radii, the zmax is between 20m to 64m AGL. In addition, results show that for all r_o, the radial V_t profile has two peaks at z<10m AGL due to strong shear force close to the ground and at higher elevation the profile transit to Rankine Combined Vortex Model (RCVM).

Keywords: Tornado wind field; CFD, Swirl ratio; tornado simulator; axisymmetric flow

1. Introduction

The tangential velocity (Vt) profile in the field can be obtained from Doppler radar measurements. Doppler radars have been used to collect the data of over 200 individual tornadoes as reported in Wurman et al. (2013). Wurman et al. (2007) asserted that due to the beam limits, the radar measurements are limited to about 20m above the ground. On the other hand, the engineers are interested at the elevations less than 10m above ground level (AGL), where the typical buildings are located. Mathematical technique of Ground-Based Velocity Track Display (GBVTD) uses data of the Doppler radar measurements to find the V_t close to the ground. Kosiba and Wurman (2010, 2013) and Refan et al. (2017) used this technique to find the tornado features of actual tornadoes. However, they reported the vertical location of the maximum V_t (zmax) occurs between 30m to 200m AGL. In addition, Nolan (2013) claimed that the close to ground V_t profile of the GBVTDs is affected by debris and thus close to ground, V_t measurements by the GBVTD are biased.

To better understand the tornadic flows, the laboratory simulators or tornado vortex chambers (TVCs) are employed. In these simulators, V_t is influenced by the following parameters as reported by Davies-Jones (1973): Reynolds number (Re), the aspect ratio (AR), and swirl ratio (S), as defined below:

$$Re = V_{ro}H_o/\nu \qquad (1)$$

Where, H_o is the inlet height of the chamber and the reference length as shown in Figure 1, V_{ro} is the radial velocity at H_o and ν is the kinematic viscosity of air. Using $Re \geq 4.5x10^4$ in the TVC models makes the tornado simulations independent of the R_e as reported by Refan et al. (2017). In addition, aspect ratio (AR) is defined as:

$$AR = H_o/r_o \qquad (2)$$

Where, r_o is the radius of the tornado or tornado simulator and is equal to half of its width. Also,

$$\text{Swirl Ratio } S = V_{to}/(2*AR*V_{ro}) = V_{to}/(2*AR*V_{ro}) \qquad (3)$$

Here V_{to} is the tangential velocity at the inlet height H_o. Equation (3) implies that S, AR, V_{ro} and r_o influence the V_{to}. That is:

$$V_{to} = 2SH_o/(r_oV_{ro})$$

In our entire write up, variables with a * like (Vt*) is the non-dimensionalized variable and without * is dimensionalized variable.

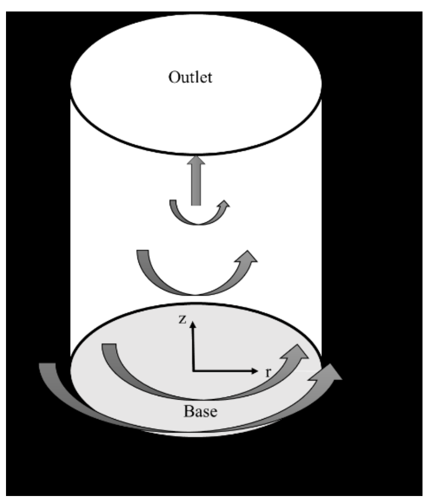

Figure 1. Schematic of a simulator and its parameters

1.1. Objective of Current Work

The major objective of this paper is to know the tornadic wind field around 10m from the ground. This will help to design low rise buildings much better and with lower susceptibility to tornadic wind hazard. The relatively small size of the laboratory simulators results in large geometric scaling ratios (Refan et al., 2017) and those simulators cannot evaluate close-to-ground V_t. In addition, the scale ratios reported by different researchers are based on either length scale or velocity scale. The length scale is calculated either using core radius r_c or location of the maximum tangential velocity z_{max} and the velocity scale is based on the maximum tangential velocity. In this work, none of the scale ratios is introduced. The detailed study conducted by Refan (2014) reports wind speed from 20 m to 80 m from the ground from both field measurements and experimental tornado simulator. Hence, it is difficult to collect wind speed around 10m from the ground using the existing data.

Well-refined computational fluid dynamics (CFD) models can compute the V_t at less than 10m AGL. Dominguez and Selvam (2017) proposed an axisymmetric CFD model to simulate a tornado chamber of 1.0km x 2.0km, where r_o=1.0km, H_o=1.0km and total height (h) =2H_o=2.0km. They used a minimum grid spacing (MGS) of 0.001H_o in the vertical axis which amounts to 1.0m from the ground for H_o=1.0km. They reported the maximum V_t occurring at less than 10m AGL. However, their study was limited to r_o=1.0km, whereas in actual tornadoes the r_o may vary. From observations of different tornadoes by National Weather Service (NWS), it can be inferred that the significant tornadoes have r_o in the range of 0.7km to 2.3km (Kashefizadeh, 2018). Therefore, the specific objectives of this research are:

1. To vary the r_o and study its influence on the maximum V_t with respect to V_{ro} and its location. Hangan and Kim (2008) and Refan (2014) showed that V_t is dependent on the S parameter and thus in order to investigate the effect of r_o on the maximum V_t, it is necessary to investigate effect of variation of S on the maximum V_t.

2. To investigate effect of r_o on less than 10m-AGL velocity profile. Typical buildings are located at elevation of z=3.3m. Therefore, the maximum V_t will be investigated at z=3.3m. Results

centered on these objectives will be highly valuable to develop recommendations for safer design of buildings.

2. Numerical Setup

Governing equations: In this study, non-dimensional Navier-Stokes equation in cylindrical coordinate system is employed using Large Eddy Simulation (LES) for an axisymmetric model. This reduces the 3D problem to 2D problem and thus reduces the computational time. Details of the equations are reported in Kashefizadeh (2018). The governing equations are non-dimensionalized using V_{ro} and H_o as the reference values. The reference value for H_o and V_{ro} are considered to be 1km and 60m/s, respectively. For these reference values, the Re will be greater than $1x10^8$.

Computational domain: The computational domain in this study is similar to the computational domain of Dominguez and Selvam (2017). Their non-dimensional computational domain is 1x2 (r_o=H_o & h=2H_o). In this study since r_o is varied from 0.7km to 2.3 km, the non-dimensional r_o* varies from 0.7 to 2.3. The increment of r_o* is 0.1, which means that r_o* will be 0.7, 0.8, 0.9 and so on.

Boundary conditions: The boundary conditions of the axisymmetric model are similar to study of Wilson and Rotunno (1986) as shown in Figure 2. For cells close to the ground, law of the wall is used as proposed by Neale et al. (2006).

2.1 Mesh of the Computational Domain:

Dominguez and Selvam (2017) used MGS=0.001H_o alongside the r- and z- axes. The present study also uses the same MGS along the r- and z-axis in the vicinity of the axisymmetric line (z-axis). Then the grid is exponentially increased by a factor of 1.1 and the maximum spacing is considered to be 0.1Ho. Figure 3 shows the computational domains for non-dimensional r_o* of 0.8 and 2. The grid sizes ranged from 46x60 to 63x60 in the r and z direction respectively.

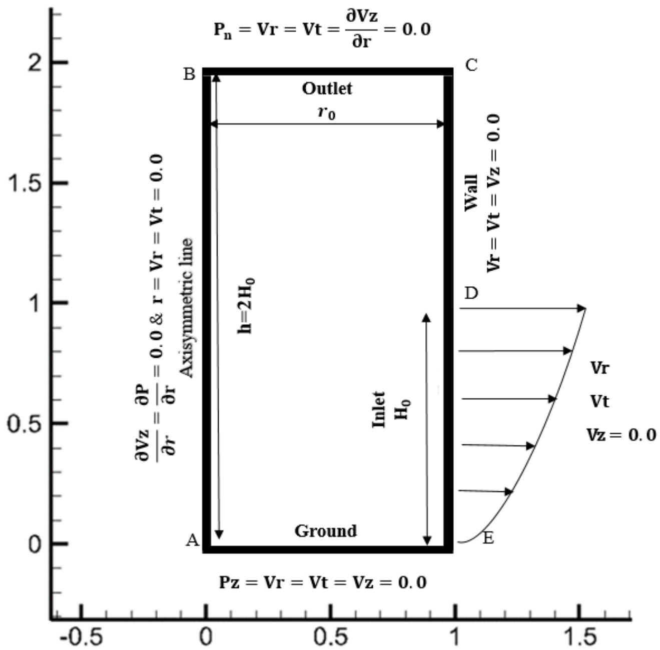

Figure 2. Axisymmetric computational domain and the boundary conditions

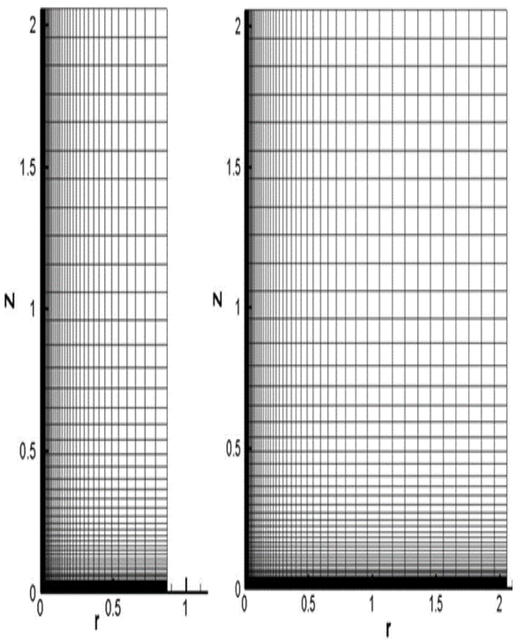

Figure 3. Computational domains for non-dimensional r_o of (a) 0.8; (b) 2.0

2.2 Radial and Tangential Velocity Components

V_r* is assumed to vary logarithmically from the ground and the equation for V_r* is as follows:

$$V_r^*(z^*)=C_1^* \ln [(z^*+zo^*)/zo^*] =C_1 \ln(1+z^*/zo^*) \quad (4)$$

For open country or Exposure C taking zo=0.035m, the non-dimensional zo* will be 0.035/1000=3.5x10^{-5}. Keeping the maximum reference V_{ro}* =1.0 the corresponding C_1 becomes:

$$C_1^*= V_{ro}^*/\ln (1+H_o^*/zo^*) = 0.0975 \quad (5)$$

Knowing V_r*(z), V_t*(z) is obtained at the inlet by rearranging Equation (3) at height z* as follows:

$$V_t^*(z^*) =[2SH_o^*Vr^*(z^*)]/r_o^* \quad (6)$$

In Equation 6, the V_r*(z*) and H_o* are constant in this work, and the two parameters S and r_o^* will be varied to determine the V_t*(z*).

2.3 Solution Scheme

The CFD model uses SOLA-Yaqui type algorithm to solve the equations (Hirt et al, 1975). In this method, a staggered grid is used where velocities are stored at the nodes and the pressure at the middle of the cell. In the momentum equation, the diffusion and convection terms are respectively implicit and explicit. All terms other than convection in the NS equations are approximated using second order finite volume method (FVM). The QUICK scheme is used for convection term. At this time, the pressure is solved using SOLA type pressure correction. The advantage of using the Yaqui-type configuration is to avoid the problem of pressure-velocity decoupling (Harlow and Welch, 1965; Selvam, 1992). The computer model is run for 5 or 10 time units with a time step of 0.1 to satisfy the CFL condition.

3. Results and Findings

3.1 Swirl ratios for Tornado Touchdown and Maximum Vt

For each r_o in the range of 0.7km to 2.3km, various S parameters in the range of 0.2 to 1.5 are used and their tornado wind-fields are investigated to determine the swirl ratio that produces the maximum V_t.

The swirl ratios affect the structure of tornadoes. Hangan and Kim (2008) and Tari et al. (2010) showed before the touchdown, S is small and tornado has a single-cell structure as shown in Figures 4 (a) and 6 (a). Then the flow slowly changes from simple jet like flow to touchdown condition. During the touchdown a vortex breakdown occurs aloft as shown in Figures 4(b) and 6 (b), and afterward the maximum V_t occurs in transition to a double-cell structure as shown in Figures 4(c) and 6 (c). To see the flow features for different r_o, r_o varying from 0.8km to 2 km are considered. Schematics of these stages are also given in Refan (2014). To see clearly, the three stages of before touchdown, at the touchdown, and double-cell structure, corresponding close up views are also shown in Figures 5 and 7. The same pattern is observed for all other r_o but not shown here.

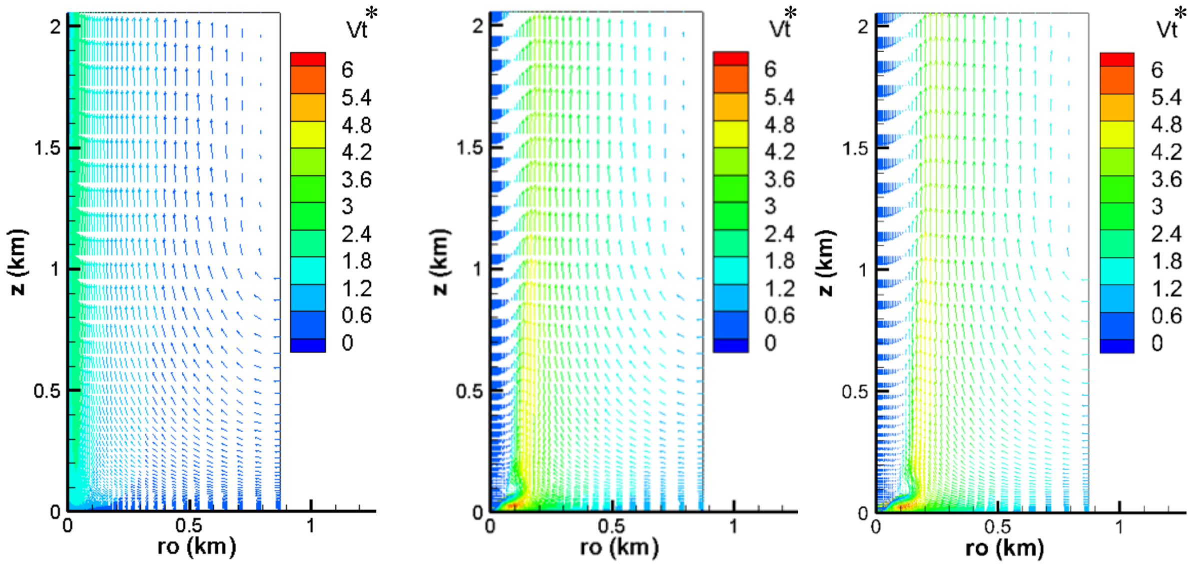

(a) (b) (c)

Figure 4. Tornado wind field for r_o=0.8km (a) S=0.3, jet-like and single-cell structure, (b) S=0.5, vortex breakdown aloft at touchdown (c) S=0.6, beyond touchdown, double-cell structure

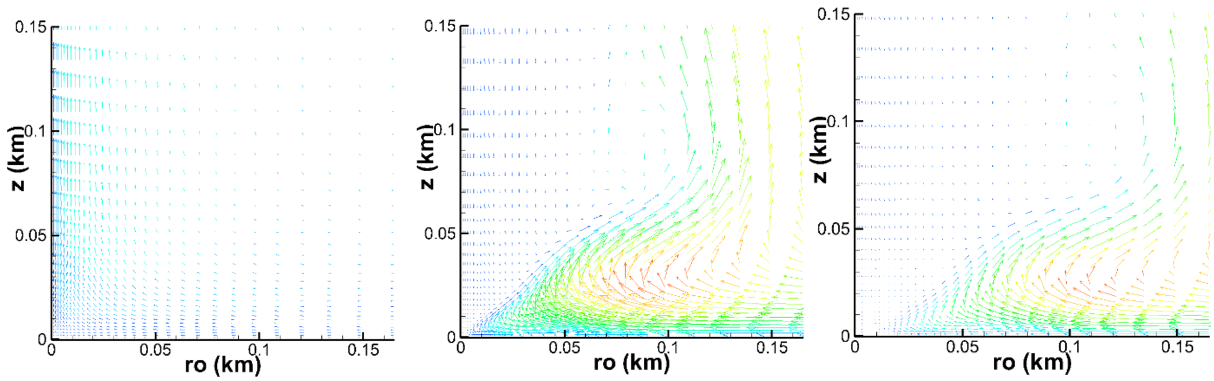

(a) (b) (c)

Figure 5. Close up view of Figure 4

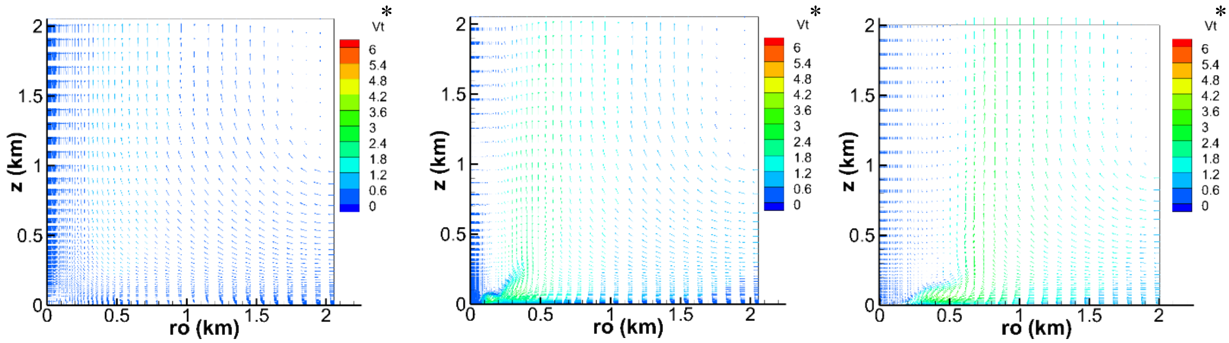

(a) (b) (c)

Figure 6. Tornado wind field for r_o=2.0km (a) S=0.3, jet-like and single-cell structure, (b) S=0.75, vortex breakdown aloft at touchdown and (c) S=1.3, beyond touchdown, double-cell structure

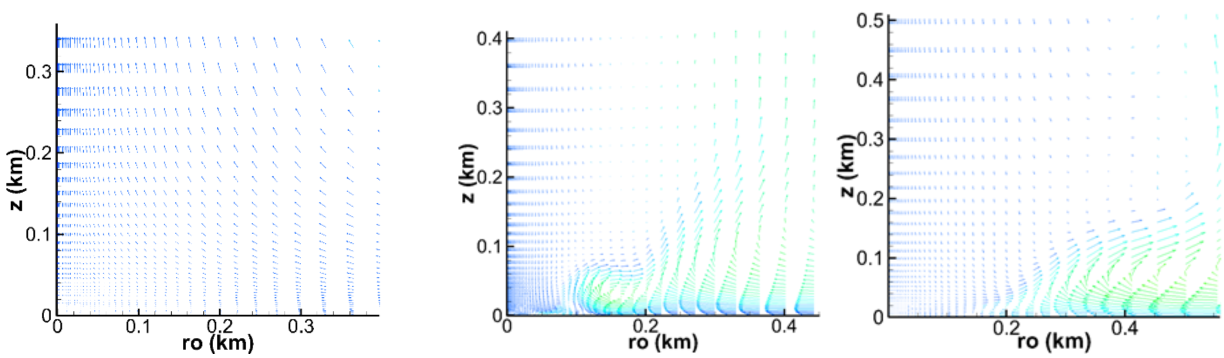

Figure 7. Close up view of Figure 6

The S for maximum V_t for each r_o is determined and plotted with S for touchdown in Figure 8. It can be seen in Figure 8 that the touchdown S increases by increasing r_o. The touchdown S is in the range of 0.40≤S≤0.9 for 0.7km≤r_o≤2.3km. Similarly, Figure 8 shows that the swirl ratio S of the maximum V_t increases by increasing r_o and is in the range of 0.50≤S≤1.2. This finding is in agreement with the previous studies where Lewellen et al (1997) suggested that by increase of r_o, the S producing maximum V_t is likely to increase. Moreover, it can be seen that the S value corresponding to that of the maximum V_t is always greater than the S value corresponding to touchdown S, which implies that the maximum V_t occurs beyond the touchdown. Therefore, in the investigation, only swirl ratios that produce tornadoes beyond touchdown are considered because these are the ones, which may affect the buildings close to the ground. Therefore, it can be concluded that for all radii, the maximum V_t occurs beyond the touchdown stage.

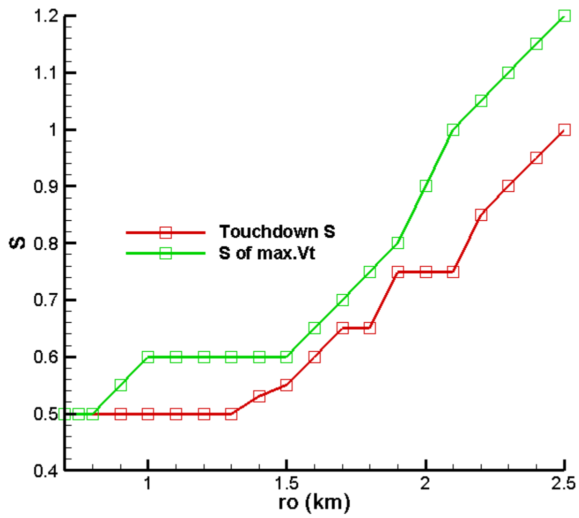

Figure 8. Swirl ratios corresponding to the touchdown and maximum V_t for $0.7km \le r_o \le 2.3km$

3.2 Effect of r_o on Maximum Vt, Core Radius (r_c) and zmax

Figure 9(a) presents the absolute maximum V_t for $0.7km \le r_o \le 2.3km$. Here on, we will call absolute maximum V_t as V_{tmax}. It can be seen in this figure that by increasing r_o from 0.7km to 2.3km, the V_{tmax} gradually reduces from $6.5V_{ro}$ to almost $3.5V_{ro}$. Likewise, Figure 9(b) shows the maximum V_t for various tornado radii at z=3.3m, which is the height of a typical low rise building and the maximum V_t gradually reduces from $2.5V_{ro}$ to almost $0.6V_{ro}$ for r_o from 0.7km to 2.3km. Similarly, Figure 9(c) shows that minimum zmax is 21m AGL for r_o=0.7km, and by increasing r_o, the zmax will also increase. However, for $r_o \ge 2.0$km, the zmax is constant at 64m. These simulations show that the zmax is in the range of 21m to 64m, whereas radar measurements report zmax in the range of 30m to 200m. Figure 9(d) presents the r_c for different r_o where r_c, is the radial distance of the location of the maximum V_t from the tornado center. It can be seen that r_c is in the range of $100m \le r_c \le 460m$ for $0.7km \le r_o \le 2.3km$. Table 1 presents a summary of the results.

Table 1 shows that for r_o=1.0km, the highest peak is $V_t=4.99V_{ro}$ at S=0.60 and zmax=28.0m. Wilson and Rotunno (1986) reported the maximum $V_t=5.0V_{ro}$ for r_o=1.0km. The reported value is for a single study of S=0.28 and zmax=1.016km. Lewellen et al. (1997) reported that for r_o=1.0km and S=0.94, the maximum V_t is $6.6V_{ro}$ at zmax= 27m AGL. Tari et al (2010) used a laboratory simulator and suggested that for r_o=1.0km, S=0.68 produces the maximum V_t at a height of 0.34ro. The difference of the results from the present study to that of Tari et al. (2010) can be due to differences in the geometry of the simulator chamber. The tornado simulator in this work is a based on Ward type, whereas the Tari et al (2010) simulator is similar to Iowa State University. The difference in the tornado chamber to touch down condition and other issues needs to be investigated further. Likewise, increase in core radius r_c with increase in chamber radius r_o is in agreement with studies of Ward (1972), Davies-Jones (1973), Jischke and Parang (1974), Church et al (1979), Church and Snow (1993), Baker and Church (1979), Tari et al. (2010), Refan (2014), and Refan et al. (2017).

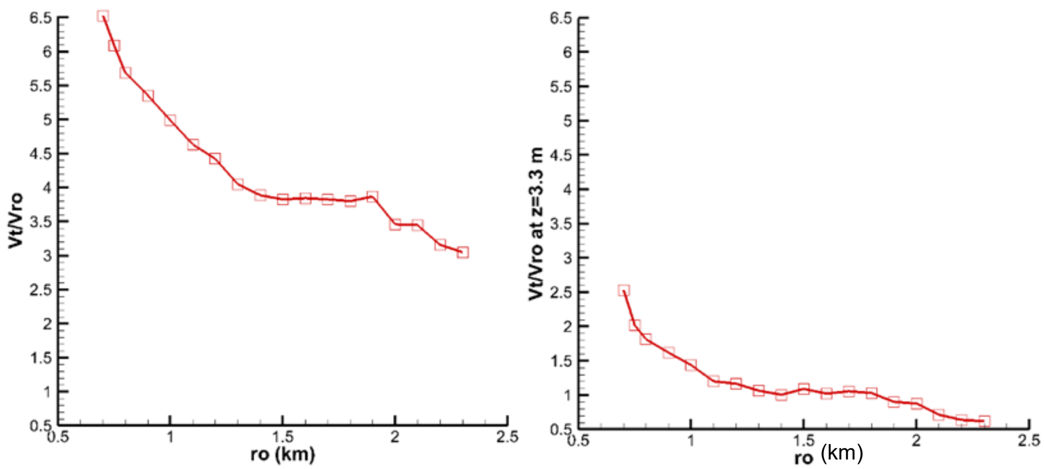

(a) (b)

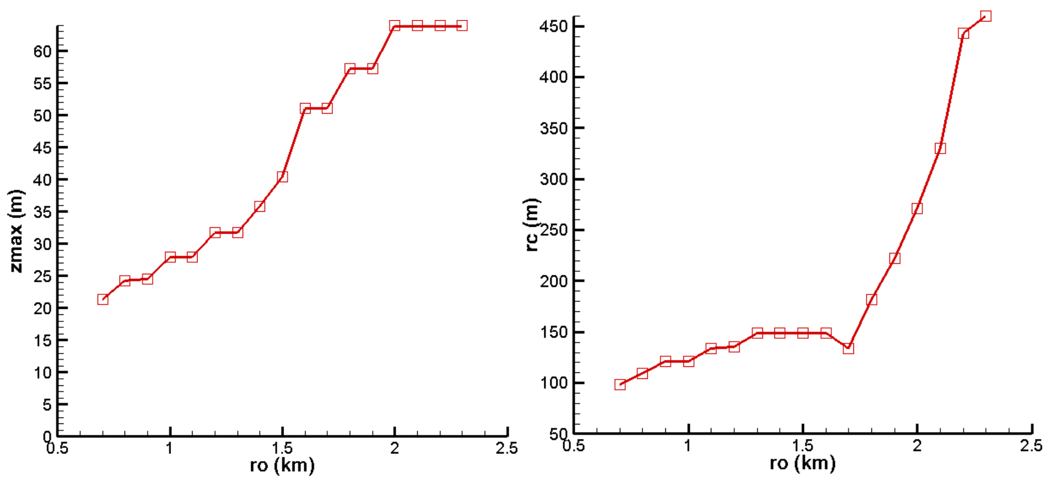

(c) (d)

Figure 9. (a) Absolute maximum V_t/V_{ro} for different r_o, (b) Maximum V_t/V_{ro} for different r_o at z=3.3m, (c) zmax of various r_o (m); and (d) Core radius of different r_o.

Table 1. Summary of the findings for different radii

r_o(km)	Touchdown S	S for V_{tmax}	V_{tmax} /V_{ro}	Max.V_t /V_{ro} at z=3.3	zmax(m)	r_c(m)
0.7	0.5	0.5	6.53	2.53	21.4	98.3
0.8	0.5	0.5	5.69	2.02	24.2	109.2
0.9	0.5	0.55	5.35	1.82	24.5	121.1
1	0.5	0.6	4.99	1.62	28	121.1
1.1	0.5	0.6	4.63	1.44	28	134.2
1.2	0.5	0.6	4.43	1.2	31.8	135.2
1.3	0.5	0.6	4.05	1.17	31.8	148.6
1.4	0.53	0.6	3.89	1.07	35.9	148.6
1.5	0.55	0.6	3.83	1.01	40.5	148.6
1.6	0.6	0.65	3.85	1.09	51.1	148.6
1.7	0.65	0.7	3.83	1.02	51.1	134.2
1.8	0.65	0.75	3.87	1.06	57.3	181.9
1.9	0.75	0.8	3.8	1.03	57.3	222.2
2	0.75	0.9	3.46	0.9	64	271
2.1	0.75	1	3.36	0.85	64	330
2.2	0.85	1.1	3.16	0.8	64	443
2.3	0.9	1.2	3.05	0.78	64	460

3.3 Effect of variation of the swirl ratio on radial V_t profiles

In this section, the effect of changing the swirl ratio on radial V_t profile is investigated. Figures 10 through 13 show the radial V_t profiles for different r_o at heights z=4.5m, z=9.5m, z=18.5m and z=51m. Figure 10 shows the radial V_t profiles at z=4.5m for r_o=0.8km, 1.5km, 1.7km, and r_o=2.0km. This figure shows that for all radii at z=4.5m, the radial V_t profile has two peaks and does not resemble the Rankine Combined Vortex Model (RCVM) profile. Also, one can see that the double curvature slowly decreases as r_o increases. Figure 11 shows the radial V_t profiles for r_o=0.8km, 1.5km, 1.7km, and 2.0km at z=9.5m. Here, for r_o greater than 0.8km, double peaks in the radial profile is distinctly observed. For r_o=0.8km, there is a slight kink close to the center. For z=18.5m and 51m, radial velocity profiles are also plotted in Figures 12 and 13. In Figure 12, slight kink is observed for higher r_o and in Figure 13 there is no double curvature at all for all radius.

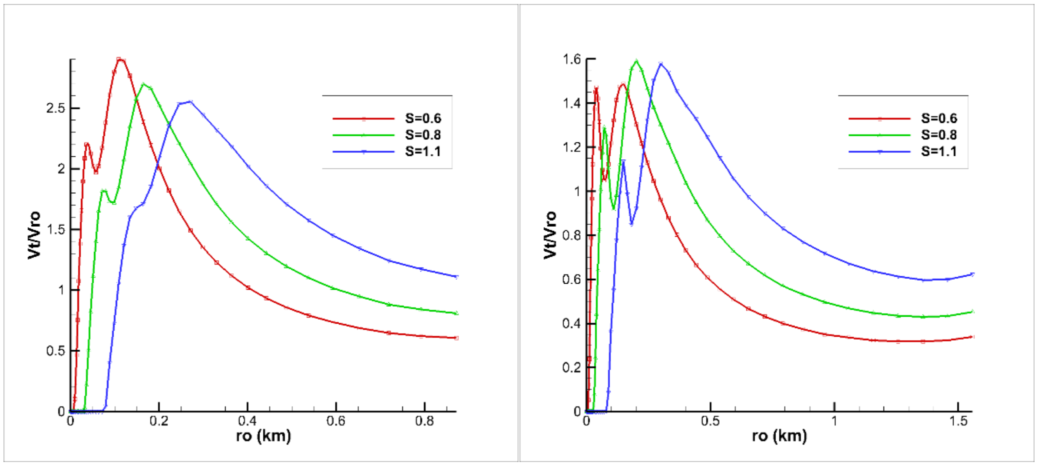

a) r_o=0.8 km b) r_o=1.5 km

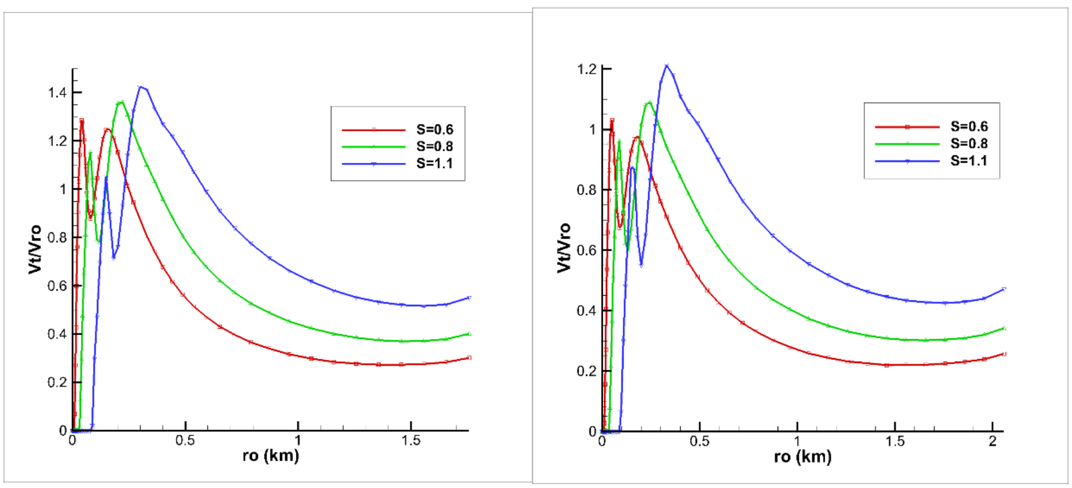

c) r_o=1.7 km d) r_o=2.0 km

Figure 10. Radial V_t profile at z=4.5m AGL for different tornado radii

Refan (2014) also showed the radial V_t profile having two peaks close to the ground in some plots. However, Refan (2014) did not make any observation. Also the peaks appeared close to the ground and away from the center in their case. These differences may be due to the way vortex chamber is built and further detailed studies are warranted. Similarly, Church et al. (1979) showed occurrence of two peaks on the velocity profile, but did not report the elevation of occurrence of the double-peak. Church et al. (1979) stated that occurrence of the secondary peak on the profile is due to the strong shear force close to the ground. It is an important observation which implies increased intensity of tornadoes close to ground. Several conclusions are made from this section:

1. For lower elevation, there are double peaks observed close to the ground for all radius ro considered in this work. When the elevation increases, the double peaks slowly disappear from smaller r_o. Therefore, wider tornadoes have higher intensity due to strong shear forces.
2. Alternatively, these observations imply that RCVM model applies for higher elevation and lower r_o.
3. For all elevations, it is noted that when the r_o decreases the maximum V_t increases or when r_o increases the maximum V_t decreases.

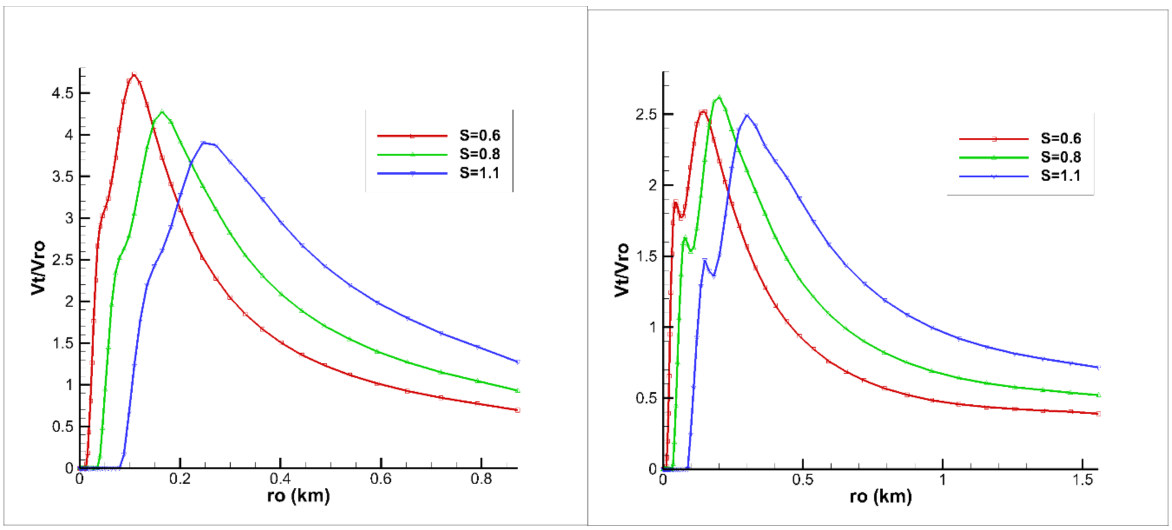

a) r_o=0.8 km b) r_o=1.5 km

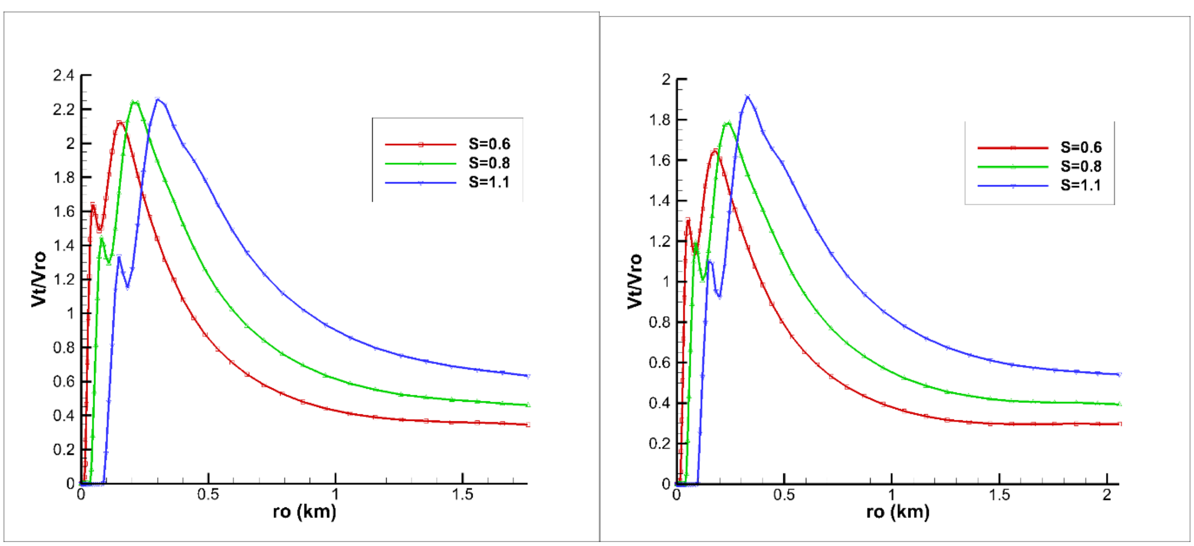

c) r_o=1.7 km d) r_o=2.0 km

Figure 11. Radial Vt profile at z=9.5m AGL for different tornado radii

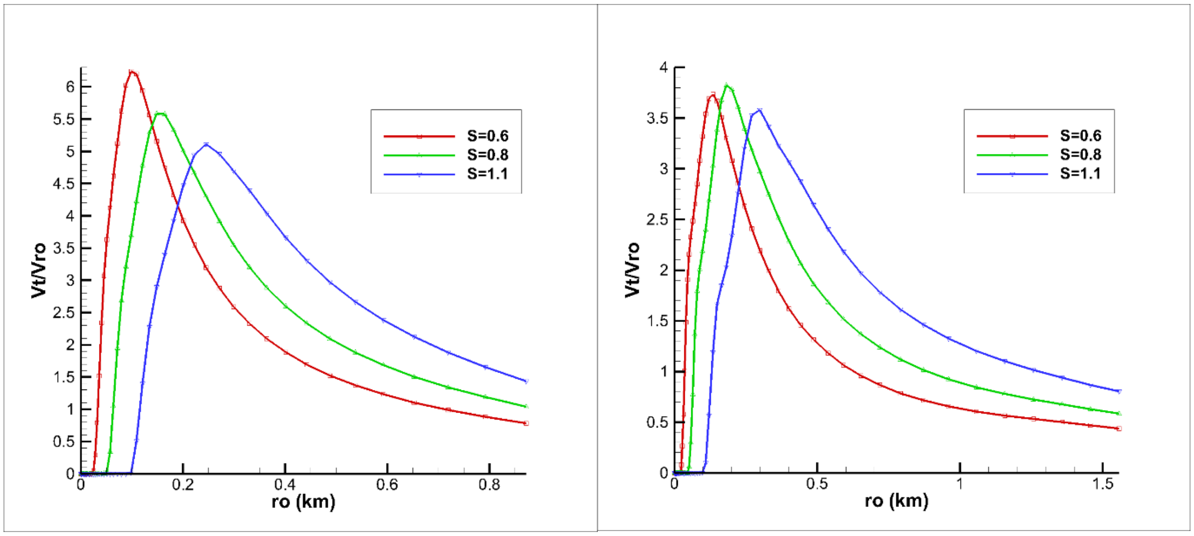

a) r_o=0.8 km b) r_o=1.5 km

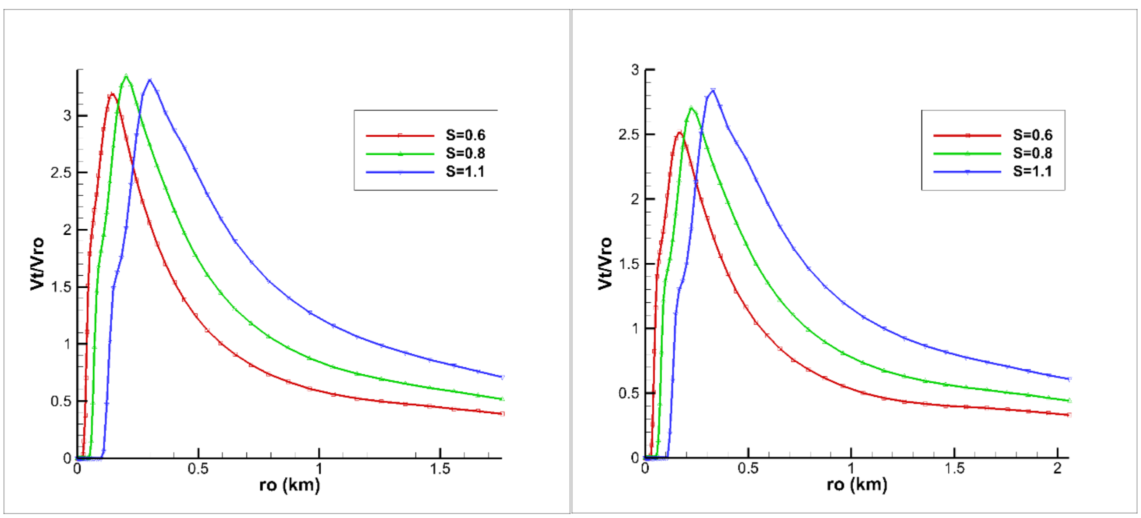

c) r_o=1.7 km d) r_o=2.0 km

Figure 12. Radial V_t profile at z=18.5m AGL for different tornado radii

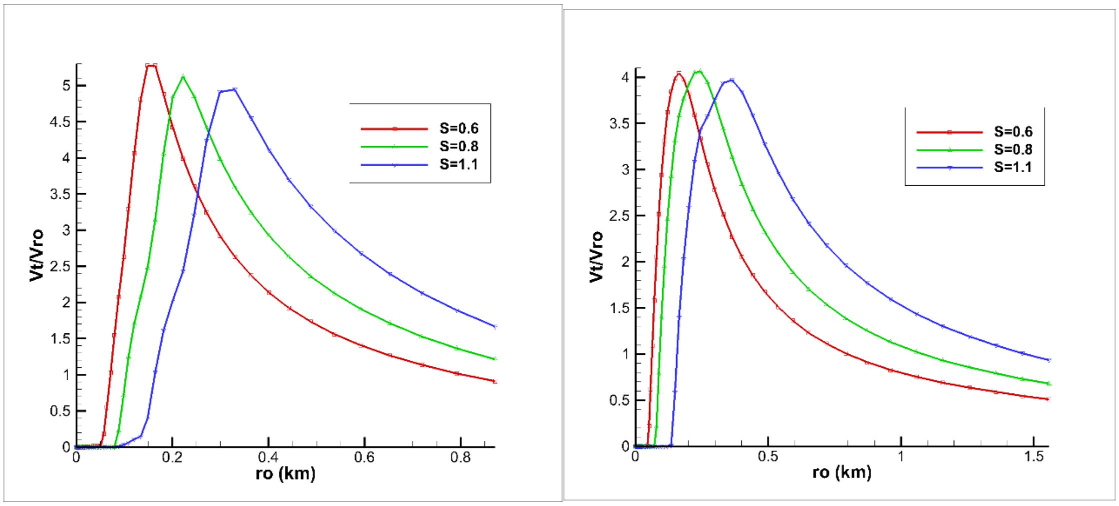

a) r_o =0.8 km   b) r_o =1.5 km

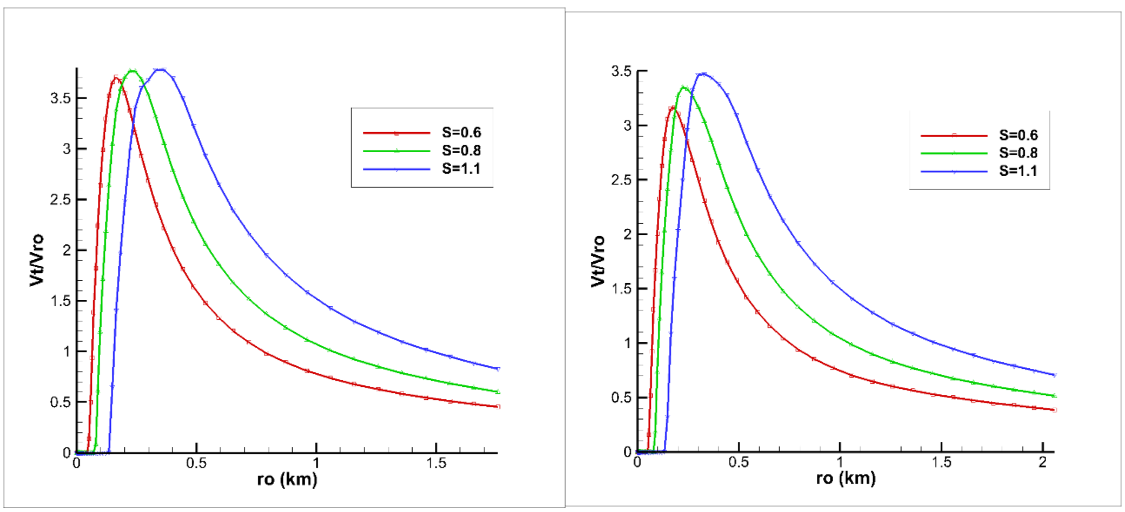

c) r_o =1.7 km   d) r_o =2.0 km

Figure 13. Radial Vt profile at z=51m AGL for different tornado radii

3.4 Comparison of Vt, r_c and zmax against the Actual Tornadoes

In this section, the simulation results will be compared against the radar measurements of actual tornadoes. For this purpose, the r_o of actual tornadoes, taken from radar measurements, are used in the simulation; the resulting tornado structure, r_c, and zmax are then compared to the data collected from actual tornadoes. This comparison is done for 6 tornadoes as shown in Table 2. Comparison of the structure of the tornadoes shows that for all 6 cases, the computational values are in the range with radar measurements. Also, comparison of r_c shows that the radar measurements report a fairly higher value than the simulations. This discrepancy is due to the debris effect in the radar measurements (Kosiba and Wurman, 2010) which causes the radars measure higher values for the r_c. The computed r_c values have error varying from 9% to 37% with respect to field observation. The error is far more for higher r_c compared to lower ones. Comparison of the zmax of the radar measurements to the simulations is possible for three actual tornadoes of Spencer, Manchester, and Goshen Wyoming tornadoes. Table 2 shows that for these three tornadoes, the zmax of simulations comply well with the actual tornadoes. Refan et al. (2017) stated that if two scaling criteria match in comparison of the simulations to the radar measurements, then the simulations are reliable. Therefore, simulation results in the present study are in close range with field measurements.

4. Conclusions

A numerical tornado simulator was proposed in order to investigate effect of the tornado radius r_o on the maximum tangential velocity V_t of tornadoes. The following conclusions are made from the simulations:

1. Increasing r_o increases the touchdown swirl ratio and the swirl ratio for maximum V_t in the range of r_o considered for simulation.

2. Increasing r_o increases zmax. For $0.7km \leq r_o \leq 2.3km$, zmax occurs in the range of $20m < zmax < 64m$, whereas the radar measurements reported zmax in the range of $30m < zmax < 200m$.

3. Investigating the maximum V_t at different elevations above and below 10m shows that an increase of r_o causes the maximum V_t to decrease with respect to V_{ro}.

4. For all r_o, at $z<10m$ AGL, the radial V_t profile has two peaks. For higher z, the double peaks in the radial profile occurs for larger r_o. In addition, these peaks appear close to the center of the chamber. This radial profile is different from RCVM flow and the detailed CFD study helped to visualize this phenomenon. However, the effect of this on force exerted on buildings is yet to be investigated. Similar double peaks were also observed by Refan (2014) but the double peaks appear away from the center and this may be due to different type of vortex chamber. Church et al. (1979) stated that occurrence of the secondary peak on the profile is due to the strong shear

force close the ground. More detailed study on the effect of different vortex chamber on double peak occurrence needs to be conducted.

5. Acknowledgements

The first author acknowledges the support received from Womble Professorship and the second and third authors acknowledges the support received from National Science Foundation, under award number CMMI-1762999. The authors acknowledge one of the anonymous reviewer comments which helped to improve the paper extensively.

Table 2. Comparison of the vertical structure, r_c and zmax of radar measurements to simulations

Tornado	r_o (km)	Technique	Structure	r_c (m)	zmax(m)
Spencer (1998)	0.8	Doppler radar (Wurman and Alexander 2005)	Double-celled	120	20
		Simulation results	Double-celled	109	21.4
Manchester (2003)	0.8	Doppler radar (Kuai et al., 2008)	Double-celled	130	20
		Simulation results	Double-celled	109	21.4
Goshen, Wyoming (2009)	1.0	Doppler radar (Wurman et al.2013)	Double-celled	140	30
		Simulation results	Double-celled	121	27.5
Dimmit, Texas (1999)	1.0	Doppler radar (Wurman and Gill, 2000)	Double-celled	150	NA
		Simulation results	Double-celled	121	27.5
El Reno (2013)	2.3	Doppler radar (Bluestein et al, 2015; Wakimoto et al. 2016)	Double-celled	650	NA
		Simulation results	Double-celled	500	65
Bridge Creek Moore(1999)	0.8	Doppler radar (Burgess et al., 2002)	Double-celled	175	NA
		Simulation results	Double-celled	110	21.4

References

Baker, G.L, Church, C.R. (1979). Measurements of core radii and peak velocities in modelled atmospheric vortices. *Journal of Atmospheric Sciences*, 36, 2413-2424.

Bluestein, H.B., Snyder, J.C., Houser, J.B. (2015). A Multiscale Overview of the El Reno, Oklahoma, Tornadic Supercell of 31 May 2013. *Weather and Forecasting*, 30, 525–552, https://doi.org/10.1175/WAF-D-14-00152.1.

Burgess, D.W., Magsig, M.A., Wurman, J., Dowell, D.C., Richardson, Y. (2002) Radar observations of the 3 May 1999 Oklahoma City tornado, *Weather and Forecasting*, 17, 456-471.

Church, C.R., Snow, J. T., Baker, G.L., Agee, E.M. (1979). Characteristics of tornado-like vortices as a function of swirl ratio: a laboratory investigation. *Journal of Atmospheric Sciences*, 36, 1755-1776.

Church, C.R., Snow, J. T. (1993). *The tornado: its structure, dynamics, prediction, and hazards*, American Geophysical Union, Washington, DC.

Davies-Jones, R.P. (1973). The Dependence of Core Radius on Swirl Ratio in a Tornado Simulator. *Journal of Atmospheric Sciences*, 30, 1427–1430.

Dominquez, D., and R.P. Selvam (2017), Tornado width for computer modeling from Google Earth data and period of the vortex, *Proceedings: AEI Conference 2017*, ASCE, Oklahoma City, OK, April 11-13, 470-483.

Hangan, H., Kim, J.D. (2008). Swirl ratio effects on tornado vortices in relation to the Fujita scale. *Wind and Structures*, 11, 291-302.

Harlow, F.H., Welch, J.E. (1965). Numerical calculation for time-dependent viscous incompressible flow of fluid with free surface. *Physics of Fluids*, 8, 2182-2189.

Hirt C.W., B.D. Nichols, and N.C. Romero, (1975). SOLA-A Numerical Solution Algorithm for Transient Fluid Flows, Los Alamos Scientific Laboratory report LA-5852.

Jischke, M. C., M. Parang, (1979). Properties of simulated tornado-like vortices. *Journal of atmospheric sciences*, 31, 506-512

Kashefizadeh, M.H. (2018). Computer Modeling of close-to-ground tornado wind-fields for different tornado widths. Master's thesis, Department of Civil Engineering, University of Arkansas, USA.

Karstens, C.D., Gallus, W.A., Lee. B.D. (2013) Analysis of Tornado-Induced Tree Fall Using Aerial Photography from the Joplin, Missouri, and Tuscaloosa–Birmingham, Alabama, Tornadoes of 2011. *Journal of Applied Meteorology and Climatology*, 52, 1049-1068.

Kosiba, K., Wurman, J. (2010). Notes and correspondence, the Three-Dimensional Axisymmetric Wind Field Structure of the Spencer, South Dakota, 1998 Tornado. *Journal of Atmospheric Sciences*, 67, 3074-3084.

Kosiba, K., J. Wurman (2013). The Three-Dimensional Structure and Evolution of a Tornado Boundary Layer, *Journal of Weather and Forecasting*. 28, 1552-1561.

Kuai, L., Haan, F.L., Gallus, W.A., Sarkar, P. (2008). CFD simulations of the flow field of a laboratory-simulated tornado for parameter sensitivity studies and comparison with field measurements. *Wind and Structures*, 11, 75-96.

Lewellen, W.S., Lewellen, D.C., Sykes, R.I. (1997). Large-eddy simulation of a tornado's interaction with the surface. *Journal of the Atmospheric Sciences*, 54, 581-605.

Neale, A., Derome, D.,Blocken, B., Carmeliet, J. (2006). CFD calculation of convective heat transfer coefficients and validation–Part 2: Turbulent flow. From the web.

Nolan, D.S. (2013). On the Use of Doppler Radar–Derived Wind Fields to Diagnose the Secondary Circulations of Tornadoes. *J. Atmos. Sci.*, 70, 1160–1171

Refan, M. (2014). Physical Simulation of Tornado-Like Vortices. PhD thesis, Department of Mechanical and Materials Engineering, The University of Western Ontario.

Refan, M., Hangan, H., Wurman, J., Kosiba, K. (2017). Doppler radar-derived wind field of five tornado events with application to engineering simulations, *Engineering Structures,* 148, 509-521.

Selvam, R.P. (1992), Computation of Pressures on Texas Tech Building, *Journal of Wind Engineering and Industrial Aerodynamics*, 43, 1619-1627.

Tari, P.H., Gurka, R., Hangan, H. (2010). Experimental investigation of tornado-like vortex dynamics with swirl ratio: The mean and turbulent flow fields. *Journal of Wind Eng. Ind. Aerodyn*. 98, 936-944.

Wakimoto, R.M., N.T. Atkins, K.M. Butler, H.B. Bluestein, K. Thiem, J.C. Synder, J. Houser, K. Kosiba, J. Wurman (2016). Aerial Damage Survey of the 2013 El Reno Tornado Combined with Mobile Radar Data. *American Meteorological Society*, 144, 1749-1776.

Ward, N.B., (1972). The exploration of certain features of tornado dynamics using a laboratory model. *Journal of the Atmospheric Sciences*, 29, 1194-1204.

Wilson, T., Rotunno, R. (1986). Numerical simulation of a laminar end-wall vortex and boundary layer. *Physics of Fluids*, 29, 3993-4005.

Wurman, J., Gill, S. (2000). Finescale Radar Observations of the Dimmitt, Texas (2 June 1995), Tornado. *Monthly Weather Review*, 128, 2135-2164.

Wurman, J. and Alexander, C.R. (2005), The 30 May 1998 Spencer, South Dakota, storm, *Monthly Weather Review*, 133, 97-119.

Wurman, J., C. Alexander, P. Robinson, Y. Richardson (2007). Low-Level Winds in Tornadoes and Potential Catastrophic Tornado Impacts in Urban Areas. *American Meteorological Society,* 89, 87-90.

Wurman, J., Kosiba, K., Robinson, P. (2013). In situ, Doppler radar and video observations of the interior structure of a tornado and the wind-damage relationship. *Bulletin of the American Meteorological Society*, 94, 835-846.